Yi et al., Expert Opin Environ Biol 2018, 7:2
DOI: 10.4172/2325-9655.1000153

Expert Opinion on Environmental Biology

Research Article

A SCITECHNOL JOURNAL

Bifurcated Response of a Regional Forest to Drought

Chuixiang Yi[1,2*], Guangwei Mu[1], George Hendrey[1,2], Sergio M Vicente-Serrano[3], Wei Fang[1], Tao Zhou[4,5], Shan Gao[1,4,5] and Peipei Xu[1,4,5]

Abstract

Several lines of evidence suggest that forest growth in many regions is declining as a consequence of changing climate. To predict the fate of forests in the future, a quantitative understanding of how the key climate variables (insolation, precipitation and temperature) interact with forests to cause the decline is a pressing need. Here we use a regionally-averaged tree-ring width index (RWI_r) to quantify forest growth in the Southwest United States (SWUS). We show that over a period of 100 years, SWUS RWI_r bifurcated into forest stands with enhanced (healthy) and reduced (declining) branches when regressed on shortwave-radiation and temperature, respectively. The reduced branch was controlled overwhelmingly by drought as measured with a regionally-averaged precipitation-evapotranspiration index ($SPEI_r$). As $SPEI_r$ approached -1.6 (previously shown as a tipping-point for SWUS conifer forest growth), RWI_r approached zero and in extreme drought years, wide spread tree mortality has been observed. Modeled trends in SPEI based on four IPCC-GHG scenarios predict SWUS $SPEI_r$ falling below -1.6 more or less continuously within a few decades. With drought expanding north- and eastward over larger areas, tree mortality may become a semi-continental phenomenon with coniferous forests transitioning to more xeric ecosystems. Our results provide insights into how to differentiate functions of climate impacts on forest growth and how to identify tipping-point control parameters for forest regime transitions.

Keywords

Forest growth decline; Tree rings; Tipping point; Bifurcation; Tree mortality; SPEI

Introduction

Forests provide an essential service in partially balancing the global carbon budget, sequestering about one quarter of anthropogenic emissions (2.4 GT C per year) [1]. However, forest health has been threatened recently by disturbances such as heat waves, persistent and extreme droughts, massive wildfire, and widespread insect outbreaks, all associated with on-going climate change [2]. In the South-western United States (SWUS) drought is a major stressor of forest ecosystems [3,4,5] leading to forest decline and there is concern that this may extend to a global phenomenon [2,3]. Particularly, regions experiencing increasing warming and drought stress are expanding and shifting to higher latitudes and altitudes [6]. As long as these on-going trends continue, forests in some regions may shift into an irreversible transition stage leading to wide-spread forest die-back resulting in substantial carbon emissions to the atmosphere.

To better understand the fate of forests over the next 100 years, we attempted to find a key climatic parameter controlling forest growth, and at what value of this control parameter the steady state of a forest ecosystem loses its stability and transitions to another stable steady state. Phase transition theory exists in physics [7-9] and ecologists have borrowed the theory to understand abrupt changes in many domains of ecological phenomena [10-12]. Particularly, forestry scientists [4,13-19] have recently become more interested in using transition theory as a power tool to tackle forest mortality issues: why and when regional forest decline occurs, and how we can identify a threshold level (tipping point) of forest growth decline. They have also realized that answering these questions qualitatively by graphics is easy but doing so quantitatively is quite challenging. The first challenge is to identify a better indicator or measurement for forest growth that also can indicate a declining trend at an early stage. Babst et al. (See Table 1 [20]) pointed out that in comparison with the other available databases (e. g. eddy-covariance fluxes, forest inventories/monitoring plots, and remote sensing images) tree-ring records have more advantages for understanding forest-climate interactions from regional to global and from year to millennial scales. Tree ring data with associated climate data, aggregated sub-regionally, allow examination of climate variability on growth at an appropriate scale, year-by-year. Regional aggregation allows the reduction of variability associated with individual trees or plots due to local edaphic conditions and permits the regional pattern to emerge. A second challenge is to identify the threshold level (tipping point) of regional forest growth decline. Distilling relationships between declining forest growth and climate parameters is the key to identifying early warning signals linked to climate trends [15]. Although forest-climate interactions have been intensively studied by observations and models over many years [21], a function descriptive of regional forest growth decline associated with a key climate control parameter remains absent [16].

To tackle these challenging questions, we have conducted a pilot study using tree-ring data and climate data for coniferous forests in the SWUS (including Arizona, New Mexico, Colorado, and Utah) over past decades. Our initial results [4] show a robust relationship between regional average tree-ring width and a standardized precipitation-evapotranspiration index (SPEI) as regional tree-ring width varies from narrow to zero. This relationship allows the prediction of a tipping point for loss of coniferous forest resistance to drought on a regional scale [22]. Here, we continue our previous studies with the same tree-ring datasets but including more climate parameters (i.e. temperature, precipitation, and short-wave radiation). The goal of this study is to distinguish what climate pattern (relationship of precipitation with temperature) provides a healthy or unhealthy condition for regional forest growth. To further understand whether SWUS coniferous forests would become unstable and pass the tipping point and shift to some alternative state with on-going climate change, we examined predicted forest growth under four different future climate scenarios. We calculated average multi-model future globally-gridded (2.5° resolution) monthly SPEI with 24 different time scales. The calculations were based on climate datasets generated by the fifth phase of the Coupled Model Intercomparison Project (CMIP5),

***Corresponding author:** Chuixiang Yi, Associate Professor, School of Earth and Environmental Sciences, Queens College of the City University of New York, New York, 11367, USA, Tel: 718-997-3366; E-mail: cyi@qc.cuny.edu

Received: February 27, 2018 **Accepted:** April 03, 2018 **Published:** April 06, 2018

with four future representative CO_2 concentration pathways (RCPs): RCP2.6, RCP4.5, RCP6.0, and RCP8.5 [23].

Materials and Methods

Focusing on SWUS conifer forests (particularly dominant species *Pinus ponderosa* and *Pinus edulis*) we used a rich tree-ring database and well-documented climate records associated with the trees sampled to develop empirical, data-driven models that: (1) identify climate patterns that reduce (or enhance) forest resistance to drought; (2) determine the potential tipping point at which regional forests lose stability and begin to shift toward another regime; and (3) predict the future regimes of SWUS forests over the rest of the twenty-first century.

RWI data

We obtained 116 chronologies of tree-ring width index (RWI) of ponderosa pine (*Pinus ponderosa*) and pinyon pine (*Pinus edulis*) within the Southwestern United States (SWUS) (Figure S1) from the International Tree-Ring Data Bank (www.ncdc.noaa.gov/paleo/treering.html), Each chronology represents the average growth of several trees (average 22 samples per site) of the same species growing at the same site. The raw RWI chronologies were standardized by employing the program AutoRegressive STANdardization, by which long-term growth trends caused by aging and increasing trunk diameter were, removed [24]. This produced unitless ring width indices (RWI) for each tree in the dataset ranging from 0 (no growth) to 2783 (maximum growth in the dataset) with a mean value for all the samples of 1000. The mean length of the chronologies used was 80 years (range 59 to 103). The time period of RWI data did not extend back in time past the year 1900 because the data of a key drought index we used, the standardized precipitation–evapotranspiration index (SPEI), are available only after that year.

SPEI data

Monthly data of SPEI with different time-scales at a spatial resolution of 0.5° were used to quantify meteorological drought conditions from 1901 to 2014. This information was obtained from the SPEIbase (http://sac.csic.es/spei/database.html) based on monthly precipitation and Penman-Monteith reference evapotranspiration from the Climatic Research Unit (CRU) of the University of East Anglia. Different SPEI time-scales (1 month to 24 month) represent cumulative water balance ranging from relatively short to long terms (e. g., SPEI obtained for time-scale of 24-month represents the cumulative water balance over the previous 24 months). SPEI is comparable in space, time and across time-scales [25,26], it is equally sensitive to changes in precipitation and the atmospheric evaporative demand [27] and has shown better performance than other drought indices in drought quantification [28] and in identification of drought impacts in a variety of sectors [29]. The SPEI values have been found to be sensitive to global warming, and identify better than other indices the strong drought events associated with the strong heat waves of 2002 in central Europe and in 2010 in Russia [26].

Climate data

Location-matched climate data (incoming shortwave radiation, temperature, and precipitation) of all tree-ring sites were retrieved from CRU+NCEP datasets downloaded at dods.extra.cea.fr/data/p529viov/cruncep/ through dgvm.ceh.ac.uk/node/9 [30-32]. The CRU+NCEP datasets are combinations of two existing datasets: (1) The UEA CRU TS3.23 dataset, which is the University of East Anglia gridded climate dataset interpolated using the original information from stations around the world for the period 1901 to 2014 [33]; and (2) US National Oceanic and Atmospheric Administration (NOAA) National Centers for Environmental Prediction (NCEP) and National Center for Atmospheric Research (NCAR) reanalysis 2.5° X 2.5° 6-hourly climatology covering the period 1948-near real time [34]. The CRU TS3.22 is 0.5-degree monthly climate data based on ground data, while the NCEP/NCAR Reanalysis is 2.5-degree 6-hourly modeled datasets. To make the CRU+NCEP datasets, the NCEP/NCAR Reanalysis was interpolated to 0.5 degree and 6-hourly variations of the interpolated NCEP/NCAR Reanalysis for each month were added to CRU TS3.22 monthly data. In this study, we used CRU+NCEP data for 6-hourly mean temperature, precipitation, and incoming shortwave radiation for the period 1901 to 2014. We made annual average or sum (e.g. precipitation) for these CRU+NCEP 6-hourly data sets.

Binned average

Based on the hypothesis that similar RWI values of ponderosa pine and pinyon pine in the SWUS were produced under similar climate conditions no matter when they were produced and where they were located, the RWI data were averaged within each of the 116 forest field sites. To remove the effects of year and site location we ranked each of the field site average RWI values across the whole region and over the 104-year period for which we had data, from the minimum to the maximum RWI values. The RWI data with their corresponding, site-specific climate data (incoming shortwave radiation, temperature, precipitation, and SPEI) were then binned as averages obtained within a moving RWI interval of 120 RWI values, incremented by 20 RWI values at each step, from RWI=0 to 2783.

RWI bifurcation model

The bifurcating relationship of RWI with the corresponding binned annual mean incoming shortwave radiation in Figure 1A can be described by an empirical model,

$$RWI = \overline{RWI} \pm \frac{\mu R_s' \Delta RWI}{\mu R_s' + \Delta RWI}, \quad (1)$$

where $\overline{RWI} = 1000$ is the mean RWI within each bin, $R_s' = R_s - \overline{R}_s$ R_s is deviation from the mean annual mean incoming shortwave radiation ($W.m^{-2}$), and is average of values that are associated with RWI values within a range [985-1015], μ is a light-ring conversion coefficient $m^2.W^{-1}$, and ΔRWI is a RWI fluctuation potential induced by climate change. The second term in Eq. (1) is a *RWI* fluctuation with amplitude given by ΔRWI and slope given by μ. A positive sign (+) is used to predict the upper branch (blue curve) with model parameter values μ=212.2 $m^2.W^{-1}$ and ΔRWI=2930, and a negative sign (-) is used to predict the lower branch with model parameter values μ=108.7 $m^2.W^{-1}$ and $\Delta RWI = 11560$.

PCA (Principle component analyses)

Principle component analyses were conducted on the correlation matrices among annual SPEI, Temperature, SW (short-wave radiation) and precipitation associated with the whole RWI dataset (WHOLE), with the upper branch of RWI bifurcation (UPPER, including all data with RWI>1000), and with the lower branch of RWI bifurcation (LOWER, including all data with RWI<1000). Then stepwise regressions were conducted using observed RWI data against the principle components of PCA, on WHOLE, LOWER and UPPER RWI dataset, respectively. As shown in the Tables S1-S3, the

coefficient of the 1st component (mostly correlated with temperature and short-wave radiation) is 20.15 for the enhanced branch, -66.125 for the reduced branch and -81.366 for the whole dataset. This suggests that RWI's response to temperature and short-wave radiation in the enhanced branch is opposite to that in the reduced branch, and such pattern will be disguised if they were not analyzed separately.

21st century SPEI scenarios

To understand whether SWUS coniferous forests would become unstable and pass the tipping point and shift toward some alternative state with on-going climate change, we calculated future globally-gridded (2.5° resolution) monthly SPEI at time scales from 1 to 24 months, based on climate datasets generated by the fifth phase of the Coupled Model Intercomparison Project (CMIP5). We calculated multi-model averages considering four future representative concentration pathways (RCPs): RCP2.6, RCP4.5, RCP6.0, and RCP8.5. Each RCP represents a level of anthropogenic radiative forcing anticipated to occur by the year 2100, ranging from 2.6 W/m^2 (RCP2.6) to 8.5 W/m^2 (RCP8.5). The SPEI data was obtained for the same reference period as the SPEI base (1901-2014) for each concentration pathway.

Results

Bifurcation of regional forest growth

Tree-ring width shows a bifurcating relationship with the corresponding binned annual mean incoming shortwave radiation, indicating two functional responses (Figure 1A). We label the upper branch enhanced growth (healthy) and the lower branch we label reduced growth (declining). It is observed that the enhanced RWI branch increases with greater incoming shortwave radiation, whereas the reduced branch is a decreasing function of incoming shortwave radiation. The explanation for this bifurcation of forest growth is that key climate variables (T,P,Rs,SPEI) are not independent and the relationships among these variables for the enhanced- and reduced-growth branches are quite different (principal component analysis, Table S1), as demonstrated below.

Our result contrasts with tree-ring-based temperature reconstructions if a correlation regression between all anomalies of tree-ring width and temperature is used, but it also shows a solution to this challenge. Temperature and tree-ring width are not correlated in a simple way (Figure 1B). There are two regimes of tree-ring width for a given temperature: wider tree-rings (green-filled circles in Figure 1B) with an enhanced growth climate (wet, higher precipitation (Figure 1C), positive SPEI (Figure 1D)) and narrow tree-rings (brown-filled circles in Figure 1B) with a reduced growth climate (dry, lower precipitation (Figure 1C), negative SPEI (Figure 1D). Our results suggest that uncertainties in temperature reconstruction will be reduced if tree-ring width data and location-matched climate data are divided into positive and negative anomaly groups and temperature is deduced by their respective regressions. Although RWI was approximately a monotonic function of precipitation under dry climate condition (see brown-filled circles in Figure 1C) the robustness of monotonicity of climate control on RWI for the reduced growth branch was dictated by SPEI (brown-filled circle in Figure 1D). SPEI is a better predictor of tree-ring growth because precipitation is only the input for the soil water balance, with soil surface evaporation, runoff, and seepage to groundwater and evapotranspiration as exports from the soil water reservoir, which are strongly determined by the atmospheric evaporative demand included in the SPEI calculations.

Different climatic features of enhanced branch from reduced growth

Figure 2A shows a similar bifurcation for the relationship of precipitation with temperature between the enhanced and the reduced growth branches. The climate associated with the enhanced growth branch is wet (SPEI>0, green-filled circles in Figure 2B) and precipitation is relatively high and nearly constant as temperature increased at the initial stage and then slightly decreased with increasing temperature (green-filled circles in Figure 2A). In contrast, the climate associated with the reduced growth branch is dry (SPEI<0, brown-filled circles in Figure 2B) and precipitation decreases almost linearly as an inverse relationship to temperature (brown-filled circles in Figure 2A). This demonstrates that high incoming solar radiation, by itself, promotes growth even in the semi-arid SWUS if water is sufficiently available (green-filled circles in Figure 2C and 2D). Tree-ring growth essentially is dependent on the water balance that is described better by SPEI (precipitation minus atmospheric evaporative demand) than by precipitation alone. Forest growth rates are substantially enhanced in hotter-wet climate but strongly reduced in hotter, drought-dominated climate. Even though the regimes of forest growth can be bifurcated by temperature, incoming shortwave radiation is a better indicator of forest growth than temperature.

The enhanced growth branch was controlled synergistically by light (incoming shortwave radiation), temperature, precipitation, and SPEI (green-filled circles in Figure 2A-2D). In the warmer condition, forest growth rate was limited mainly by light and temperature (green-filled circles in Figure 1A-1B) due to maintenance of a consistently high level of soil moisture. In contrast, the changes in forest growth rate on the reduced growth branch are controlled primarily by soil moisture (brown-filled circles in Figure 2A-2D) even though there is a strong correlation between RWI and annual mean incoming shortwave radiation (Figure 1A). The reduced growth climate (red curve in Figure 2B) is characterized by warmer and drier conditions with high light intensity. Although the effect of warmer temperature on heat stress with increased evapotranspiration leading to hydraulic failure [36,37] cannot be ruled out as a contributor to forest growth decline, this would be related to insufficient soil moisture, which appears to be an underlying reason for forest growth reduction.

Quantifying the approach to a tipping point

Tree-ring width can be considered as an indicator of tree vitality [38,39], reflecting forest growth potential. Living trees that have zero ring-growth are functioning near to or below their physiological compensation point, but if climate conditions improve the tree may recover and exhibit growth again. When trees do die of drought, tree ring growth is generally quite reduced prior to death [38-41]. The evidence leads us to hypothesize that regional forest growth potential can be measured by regional average tree-ring width (RWI). Narrow average tree-ring width, relative to normal growth, reflects stress, with lowered capacity for survival, lower ability to recover, and more vulnerability to attack by insects and pathogens.

The idea of forest growth or capacity for survival can be illustrated following Scheffer's concept of a corresponding basin of attraction [42] (Figure 1E) Wider tree-ring width indicating a healthy forest implies that the basin of attraction of a forest regime is deep. For a healthy forest (e.g. the enhanced growth branch in Figure 1A), relationships between forest growth potential and climate drivers is complicated. Under conditions of sufficient soil moisture, forest growth potential was synergistically controlled by light and temperature (green-filled

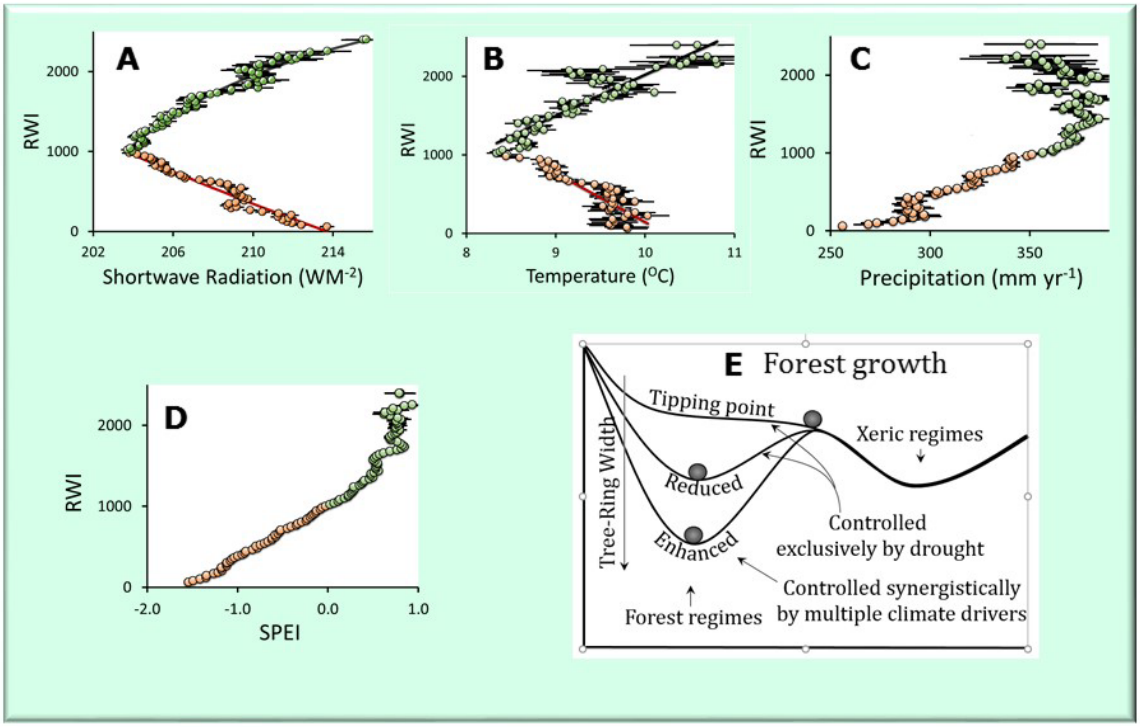

Figure 1: Binned RWI versus associated binned climate drivers: (A) annual mean incoming shortwave radiation; (B) annual mean temperature; (C) annual precipitation; and (D) SPEI. A conceptual model of forest growth is summarized in (E). The filled green circles are binned RWI values above the average (1000), while the filled brown circles below the average. The vertical bar on each point is the standard error of binned RWIs and horizontal bar on each point is the standard error of binned climate drivers.

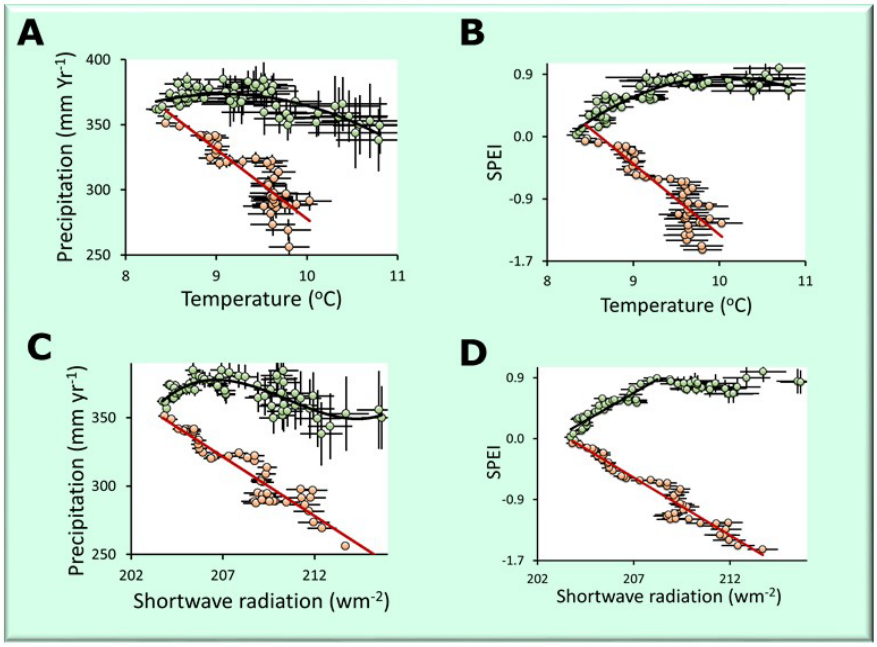

Figure 2: Climate patterns of SWUS coniferous forest resistance: (A) precipitation versus temperature; (B) SPEI versus temperature; (C) precipitation versus shortwave radiation; and (D) SPEI versus shortwave radiation. All these climate data were binned in the same way as their associate binned RWIs. The filled green circles reveal climatic patterns (relationships) associated with the enhanced forest resilience branch, while filled brown circles reveal climatic patterns (relationships) associated with the reduced forest resilience branch. The vertical bar on each point is the standard error of binned precipitations (A and C) and that of binned SPEIs in (B and D), and horizontal bar on each point is the standard error of binned annual mean temperatures (A and B) and of binned annual mean shortwave radiation (C and D).

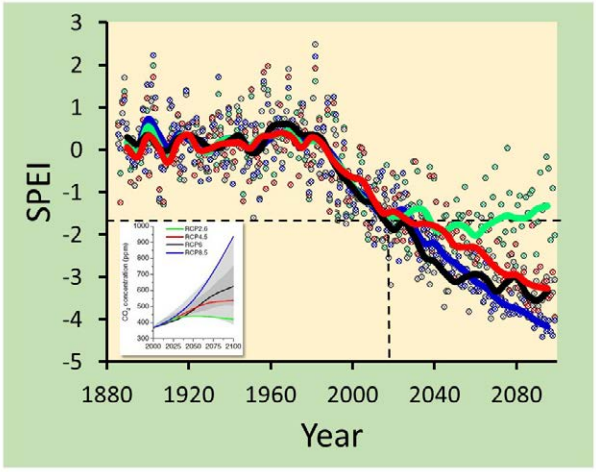

Figure 3: Future prediction of regional average SPEI in SWUS. Future SPEI data with globally-gridded (2.5° resolution) monthly SPEI with 24 different time scales [5] are calculated based on climate datasets generated by CMIP5 with four future representative concentration pathways: RCP2.6, RCP4.5, RCP6.0, and RCP8.5 (equivalent CO_2 concentrations of four RCPs shown at bottom-left). The data points are average values of July SPEI with 11-month time scale over SWUS whole region (framed area in Figure S1) for the four RCP scenarios. The dashed line indicates when SWUS would approach the tipping point identified in Figure 1d.

circles in Figure 1A-1D). For a reduced growth climate, relationships between forest growth potential and climate drivers became simpler, controlled overwhelmingly by drought (Figure 1D).

As drought becomes more severe (SPEI more negative), growth potential as indicated by RWI decreases almost linearly towards a tipping point that is defined by zero radial growth at SPEI=(-1.60) (Figure 1D). The tipping point does not mean that all trees must die, but that the forest is vulnerable to drought and struggling to survive (e. g. missing ring) [22,43]. The SWUS experienced an extreme drought event in 2002 and the regional average SPEI (-1.79) passed the tipping point, accompanied by the death of 225 million trees [44,45]. Empirically, SPEI seems a good indicator to measure the distance of the forest growth potential from the tipping point.

The future of SWUS coniferous forests

To understand whether SWUS coniferous forests would become unstable and pass the tipping point, then shift to some alternative state with on-going climate change, we examined predicted forest growth under four different future climate scenarios. We calculated average multi-model future globally-gridded (2.5°resolution) monthly SPEI with 24 different time scales. The calculations were based on climate datasets generated by the fifth phase of the Coupled Model Intercomparison Project (CMIP5), with four future representative concentration pathways (RCPs): RCP2.6, RCP4.5, RCP6.0, and RCP8.5 [23]. Each RCP represents a level of anthropogenic radiative forcing anticipated to occur by the year 2100, ranging from 2.6 W/m^2 (RCP2.6) to 8.5 W/m^2 (RCP8.5). Figure 3 shows that the projected trends of SWUS regional average SPEIs under these CMIP5 RCP scenarios are consistent, declining from the 1980s and approaching the tipping point around 2020. Only SPEI RCP2.6, a mitigation scenario aimed to limit the increase of global mean temperature to 2°C, will limit the ongoing trend toward the tipping point near the end of 21st century. The other three SPEI RCPs exhibit persistent multi-decadal drying trends surpassing the tipping point towards the end of 21st century.

The overall drying trend of SWUS from 1980s to 2100 shown by SPEI in Figure 3 is in agreement with studies by soil moisture metrics analyses from 21st century climate models [35,46], resulting from decreased precipitation driven by a poleward shift of the subtropical dry zone associated with the descending branch of the expanding Hadley cell 6 and the increasing anticyclonic conditions [47] and by increased atmospheric evaporative demand [3]. From 1980 to the present, SWUS has been accelerating into a prolonged drier era (Figure 3). Our analyses based on the CMIP5 RCP scenarios predicts that this will continue and soon will result in the loss of coniferous forest growth potential and the transition to a condition perhaps similar to the Sonoran Desert (Figure 1E). In fact, an unusual amount of tree mortality associated with the drying trend already has been reported. McDowell et al. [3] used the predawn leaf water potential model to predict that 72 % of SWUS coniferous forests will experience mortality by 2050, with nearly 100% forest mortality by 2100.

Discussion

Forest growth may be determined by many abiotic and biotic factors [16]. Our results strongly suggest that the SWUS forest growth stability basin (Figure 1E) is becoming shallower, overwhelmingly driven by soil moisture and atmospheric evaporative demand under hotter and drier climate conditions. With projected climate changes it should be expected that during this century the SWUS region largely will 'tip' into a variety of alternative xeric states from which it will be difficult to recover.

Anthropogenic warming is producing co-occurring warm-dry conditions [48] that are expanding not only throughout the SWUS but also deeper into North America [6,49]. In-situ observations from the world-wide tower network (FLUXNET) demonstrate that CO_2 transfer from the atmosphere to terrestrial ecosystems in land areas that are warm (annual average >16°C) is limited mainly by dryness [50]. As forests die, not only will their atmospheric CO_2 uptake decline but also the carbon stored in the wood and soils will be released to the atmosphere. More xeric ecosystems replacing the conifer forests will have a lower standing stock and biomass. Reduced CO_2 uptake and storage will have a positive feedback on global climate change that is likely to accelerate the rate of climate warming and forest dieback [51].

Employing regional average tree-ring width data as an indicator of forest growth, as demonstrated in this study, would be useful in understanding of potential collapse of regional forests with the warming climate trend and could contribute to improved predictive models of global climate change. In addition, the bifurcation of forest growth is a new tool that can be used to open up a novel avenue of research in dendroclimatic reconstruction.

Acknowledgments

CY was supported by City University of New York, PSC-CUNY ENHC-48-33 and PSC-CUNY CIRG- 80209-08 22. The authors thank two anonymous reviewers for their constructive comments.

References

1. Pan Y, Birdsey RA, Fang J, Houghton R, Kauppi PE, et al. (2011) A large and persistent carbon sink in the world's forests. Science 333: 988-993.
2. Allen CD , Breshears DD, McDowell NG (2015) On underestimation of global vulnerability to tree mortality and forest die-off from hotter drought in the Anthropocene. Ecosphere 6: 129.
3. McDowell NG, Williams AP, Xu C, Pockman WT, Dickman LT, et al. (2015) Multi-scale predictions of massive conifer mortality due to chronic temperature rise. Nat Clim Change 6: 295-300.

4. Huang K, Yi C, Wu D, Zhou T, Zhao X, et al. (2015) Tipping point of a conifer forest ecosystem under severe drought. Environ Res Lett 10: 024011.

5. Williams AP, Allen CD, Macalady AK, Griffin D, Woodhouse CA, et al (2013) Temperature as a potent driver of regional forest drought stress and tree mortality. Nat Clim Change 3: 292-297.

6. Yi C, Wei S, Hendrey G (2014) Warming climate extends dryness-controlled areas of terrestrial carbon sequestration. Sci Rep 4: 5472.

7. Nicolis G, Prigogine I (1977) Self-organization in non-equilibrium system: from dissipative structures to order through fluctuations. John Wiley & Sons, Inc., New York.

8. Haken H (1983) Synergetics: An Introduction, (3rd edtn), Springer, Berlin.

9. Thom R (1975) Structural Stability and Morphogenesis. Bull Math Biol 39: 629-632.

10. Scheffer M (2009) Critical Transitions in Nature and Society. Princeton University Press.

11. Holling CS (1986) The resilience of terrestrial ecosystems: local surprise and global change: Sustainable Development of the Biosphere. Cambridge University Press, Cambridge, U.K.

12. Rockstrom J, Steffen W, Noone K, Persson A, Chapin III FS, et al (2009) A safe operating space for humanity. Nature 461: 472-475.

13. Millar CI, Stephenson NL (2015) Temperate forest health in an era of emerging megadisturbance. Science 349: 823-826.

14. Trumbore S, Brando P, Hartmann H (2015) Forest health and global change. Science 349: 814-818.

15. Camarero JJ, Gazol A, Sanguesa-Barreda G, Oliva J, Vicente-Serrano SM (2015) To die or not to die: early warnings of tree dieback in response to a severe drought. J Ecol 103: 44-57.

16. Reyer CPO, Brouwers N, Rammig A, Brook BW, Epila J, et al. (2015) Forest resilience and tipping points at different spatio-temporal scales: approaches and challenges. J Ecol 103: 5-15.

17. Ghazoul J, Burivalova Z, Garcia-Ulloa J, King LA (2015) Conceptualizing forest degradation. Trends Ecol Evol 30: 622-632.

18. 18. Helman D, Lensky IM, Yakir D, Osem Y (2017) Forests growing under dry conditions have higher hydrological resilience to drought than do more humid forests. Global Change Biol 23: 2801-2817.

19. Gazol A, Camarero JJ, Vicente-Serrano SM, et al. (2018) Forest resilience to drought varies across biomes. Glob Chang Biol 24: 2143-2158.

20. Babst F, Alexander MR, Szejner P, Bouriaud O, Klesse S, et al. (2014) A tree-ring perspective on the terrestrial carbon cycle. Oecologia 176: 307-322.

21. Bonan GB (2008) Forests and climate change: forcings, feedbacks, and the climate benefits of forests. Science 320: 1444-1449.

22. Kolb TE (2015) A new drought tipping point for conifer mortality. Environ Res Lett 10: 031002.

23. Moss RH, Edmonds JA, Hibbard KA, Manning MR, Rose SK, et al. (2010) The next generation of scenarios for climate change research and assessment. Nature 463: 747-756.

24. Cook ER, Kairiukstis LA (1990) Methods of Dendrochronology: Applications in the Environmental Sciences. Springer, Dordrecht, Netherlands.

25. Vicente-Serrano SM, Begueria S, Lopez-Moreno JI (2010) A multiscalar drought index sensitive to global warming: The standardized precipitation evapotranspiration index. J Clim 23: 1696-1718.

26. Begueria S, Vicente-Serrano SM, Reig F, Latorre B (2014) The Standardized Precipitation Evapotranspiration Index (SPEI) revisited: parameter fitting, evapotranspiration models, kernel weighting, tools, datasets and drought monitoring system. Int J Climatol 34: 3001-3023.

27. Vicente-Serrano SM, Van der Schrier G, Begueria S, Azorin-Molina C, Lopez-Moreno JI, et al. (2015) Contribution of precipitation and reference evapotranspiration to drought indices under different climates. J Hydrol 426: 42-54.

28. Vicente-Serrano SM, Begueria S, Lopez-Moreno JI (2011) Comment on "Characteristics and trends in various forms of the Palmer Drought Severity Index (PDSI) during 1900-2008" by A Dai. J Geophys Res Atmos 116.

29. Vicente-Serrano SM, Begueria S, Lorenzo-Lacruz J, Camarero JJ, Lopez-Moreno JI, et al. (2012) Performance of drought índices for ecological, agricultural and hydrological applications. Earth Interact 16: 1-27.

30. New M, Hulme M, Jones P (2000) Representing twentieth-century space-time climate variability. Part II: Development of (1901-1996) monthly grids of terrestrial surface climate. J Clim 13: 2217-2238.

31. New M, Lister D, Hulme M, Makin I (2002) A high-resolution data set of surface climate over global land areas. Clim Res 21: 1-25

32. Kalnay E, Kanamitsu M, Kistler R, Collins W, Deaven D, et al (1996) The NCEP/NCAR 40-Year Reanalysis Project. Bull Am Meteorol Soc 77: 437-471.

33. Harris I, Jones PD, Osborn TJ, Lister DH (2014) Updated high-resolution grids of monthly climatic observations-the CRU TS3.10 Dataset. Int J Climatol 34: 623-642.

34. Fisher JB, Sikka M, Sitch S, Ciais P, Poulter B, et al. (2013) African tropical rainforest net carbon dioxide fluxes in the twentieth century. Philos Trans R Soc Lond B Biol Sci 368: 20120376.

35. Cook BI, Ault TR, Smerdon JE (2015) Unprecedented 21st century drought risk in the American Southwest and Central Plains. Sci Adv 1: e1400082.

36. Sulman BN, Roman DT, Yi K, Wang L, Phillips RP, et al (2016) High atmospheric demand for water can limit forest carbon uptake and transpiration as severely as dry soil. Geophys Res Lett 43: 9686-9695.

37. Mu Q, Zhao M, Running SW (2011) Improvements to a MODIS global terrestrial evapotranspiration algorithm. Remote Sens Environ 115: 1781-1800 .

38. Dobbertin M (2005) Tree growth as indicator of tree vitality and of tree reaction to environmental stress: a review. Eur J For Res 124: 319-333.

39. Grote R, Gessler A, Hommel R , Poschenrieder W, Priesack E (2016) Importance of tree height and social position for drought-related stress on tree growth and mortality. Trees 30: 1467-1482.

40. Bigler C, Gavin DG, Gunning C, Veblen TT (2007) Drought induces lagged tree mortality in a subalpine forest in the Rocky Mountains. Oikos 116: 1983-1994.

41. Kane JM, Kolb TE (2014) Short- and long-term growth characteristics associated with tree mortality in southwestern mixed-conifer forests. Can J Forest Res 44: 1227-1235.

42. Scheffer M, Carpenter S, Foley JA, Folke C, Walker B (2001) Catastrophic shifts in ecosystems. Nature 413: 591-596.

43. Clifford MJ, Royer PD, Cobb NS, Breshears DD, Ford PL (2013) Precipitation thresholds and drought-induced tree die-off: Insights from patterns of Pinus edulis mortality along an environmental stress gradient. New Phytol 200: 413-421.

44. Hicke JA, Meddens AJH, Kolden CA (2016) Recent tree mortality in the western United States from bark beetles and forest fires. For Sci 62: 141-153.

45. Anderegg WRL, Flint A, Huang CY, Flint L, Berry JA, et al. (2015) Tree mortality predicted from drought-induced vascular damage. Nat Geosci 8: 367-371.

46. Seager R, Ting M, Held I, Kushnir Y, Lu J, et al. (2007) Model projections of an imminent transition to a more arid climate in south-western. Science 316: 1181-1184.

47. Prein AF, Holland GJ, Rasmussen RM, Clark MP, Tye MR (2016) Running dry: The US Southwest's drift into a drier climate state. Geophys Res Lett 43: 1272-1279.

48. Diffenbaugh NS, Swain DL, Touma D (2015) Anthropogenic warming has increased drought risk in California. Proc Natl Acad Sci 112: 3931-3936.

49. Pravalie R (2016) Drylands extent and environmental issues: A global approach. Earth Sci Rev 161: 259-278.

50. Yi C, Ricciuto D, Li R, Wolbeck J, Xu X, et al. (2010) Climate control of terrestrial carbon exchange across biomes and continents. Environ Res Lett 5.

51. Yi C, Pendall E, Ciais P (2015) Focus on extreme events and the carbon cycle. Environ Res Lett 10: 070201.

Author Affiliations

Top

[1]*School of Earth and Environmental Sciences, Queens College of the City University of New York, New York, 11367, USA*

[2]*Department of Earth and Environmental Sciences, the Graduate Center of the City University of New York, New York, NY 10016, USA*

[3]*Instituto Pirenaico de Ecología, Consejo Superior de Investigaciones Cientificas (IPE-CSIC), Zaragoza 50080 Spain*

[4]*State Key Laboratory of Earth Surface Processes and Resource Ecology, Beijing Normal University, Beijing 100875, China*

[5]*Academy of Disaster Reduction and Emergency Management, Faculty of Geographical Science, Beijing Normal University, Beijing 100875, China*